ISSN 2176-5480

22nd International Congress of Mechanical Engineering (COBEM 2013)
November 3-7, 2013, Ribeirão Preto, SP, Brazil

ROTOR FAULTS IDENTIFICATION USING CORRELATION ANALYSIS AND MODEL ORDER REDUCTION

Fabio Dalmazzo Sanches[1]
Robson Pederiva[2]
[1] Universidade Federal do Rio Grande do Norte, Campus Universitário, Centro de Tecnologia: Departamento de Engenharia Mecânica, Av. Senador Salgado Filho S/N, CEP: 59072-970, Natal-RN.
[2] Universidade Estadual de Campinas, Faculdade de Engenharia Mecânica, Cidade Universitária Zeferino Vaz, CEP: 13083-860, Campinas-SP.
dalmazzo@ct.ufrn.br [1], robson@fem.unicamp.br[2]

Abstract. *Fault identification is a matter that involves many researchers and industries around the world due its economic importance, since malfunction or, in an extreme case, a complete stop of the equipment leads to high financial losses. This paper proposes an identification methodology based on the mathematical models of the rotor and the fault to estimate the fault related parameters. Theoretical studies are performed for a Jeffcott rotor which is modeled by finite elements. Using state space representation and the definition of correlation matrix, it is possible to obtain an estimator in time domain that involves the rotor parameters, the fault parameters and the simulated rotor outputs. Finite element model is reduced by Guyan method in order to enable the algorithm through the lowering of the observability matrix order. The analyzed fault is the unbalance present at the rotating disc and the goal is to quantify and locate this fault using only the rotor outputs. Simulated initial results are considered good and show a way to the validation in a test rig.*

Keywords: *Rotordynamics, Correlation Analysis, Guyan Reduction, Faults Identification*

1. INTRODUCTION

Rotating machinery is a basic part in any industry. In real systems, faults are inevitable due to errors in manufacturing, provision of tolerances on mating parts, errors while assembling different parts of the system and if they are not significant in magnitude initially, faults may develop in the system due to the operating conditions such as heat generation, looseness, wear, etc. Failure of the rotor system has safety implications along with economical considerations (Sudhakar and Sekhar, 2011).

In general, two main approaches can be used to identify faults in rotating machines. In the first approach, the symptoms can be defined using qualitative information, based on human operator´s experience, which creates a knowledge base: expert systems, fault-symptom matrices, fault-symptom trees, fuzzy logic classification and artificial neural networks (ANN) can be used in the identification process. The second approach is quantitative and is called model-based fault detection method in which a reliable model of the system is used to create an input-output relation (Baschschmid *et al.,* 2002).

Generally, the models have the same goal but they are different in mathematical approach and inclusion/representation of parts of the complete system: bearings, foundations, seals, etc. The advantage of this approach is the fault identification without using trial masses or test running. A general overview of model-based identification can be seen in Lees *et al.* (2009).

Many researchers have successfully identified rotor faults using model based methods. Market *et al.* (2001) identified rotor faults using virtual loads generated in the system due the faults. Sekhar (2005) used this approach for the identification of unbalance and crack occurring simultaneously. Baschschmid *et al.* (2002) identified multiple faults by means of minimization of a multidimensional residual between vibrations in some measuring planes on the machine and calculated vibrations due to the acting faults. Jalan and Mohanty (2009) identified unbalance and misalignment experimentally in a rotor bearing system using model based method.

The methodology proposed in this paper uses the Lyapunov matrix equation and correlation analysis without the measuring of the input signals. The interest parameters are estimated from the correlations among the measured degrees of freedom. In rotor dynamics field, this method was used with white noise excitation and lumped mass matrix (Pederiva, 1992), unbalance plus stochastic input forces and artificial neural network to identify the fault parameters (Eduardo, 2003), random input and finite elements modeling to identify the bearing parameters (Sanches and Pederiva, 2009), harmonic (unbalance) input in order to identify the fault parameters (Sanches and Pederiva, 2010) and the presence of unbalance and shaft bow occurring simultaneously at two rotating discs. These faults were successfully identified and located (Sanches and Pederiva, 2011). In these last two papers, it was used lumped mass matrix.

This paper utilizes finite elements (distributed-parameter matrices) to have an accurate model of the rotating system. State space representation is used to generate the correlation matrices between the rotor outputs and the unbalance parameters. A coordinate change, based on the observability matrix, is performed in order to reduce the system order.

ISSN 2176-5480

Depending on the degree of this reduction, the observability matrix has high powers of the system matrix and the reduction cannot be performed.

In order to low the powers involved in the generation of the observalibily matriz and the computational cost, the system model should be reduced. A good survey and review of model reduction methods and their application to rotor dynamic systems can be found in Wagner *et al.* (2010) and Rades (2009).

The initial studies presented here deal with the unbalance identification using the simplest model order reduction method: the Guyan reduction, since there are not so many papers using model order reduction to identify failures in rotating machines

2. MATHEMATICAL MODELLING

Considering that the rotor-bearing system, which is excited by harmonic forces due to unbalance and residual bow, can be modeled by a linear and time invariant mechanical system with *n* degrees of freedom, then the differential matrix equation that describes the physical system is (Rao, 2001):

$$[M]\{\ddot{\xi}(t)\}+[P]\{\dot{\xi}(t)\}+[K]\{\xi(t)\}=[H]\{n_1(t)\} \tag{1}$$

where [*M*] is the mass matrix, [*P*] is a matrix of speed proportional forces, [*K*] is a matrix of displacements proportional forces, $\{\xi(t)\}$, $\{\dot{\xi}(t)\}$ and $\{\ddot{\xi}(t)\}$are the vectors corresponding to displacements, velocities and accelerations in this order, [*H*] is the unbalance matrix, [*B*] is the bow matrix.

The vector $\{n_1(t)\}$ is the harmonic vector referent to unbalance. It can be expressed as:

$$\{n_1(t)\}=\begin{Bmatrix}\sin(\Omega t+\beta)\\ \cos(\Omega t+\beta)\end{Bmatrix} \tag{2}$$

where Ω is the rotating frequency and β is the unbalance phase.

The matrix [*H*] can be given by:

$$[H]=\begin{bmatrix}0 & 0\\ \vdots & \vdots\\ m_u d\Omega^2 & 0\\ 0 & m_u d\Omega^2\\ 0 & 0\\ \vdots & \vdots\\ 0 & 0\end{bmatrix}_{(n,2)} \tag{3}$$

m_u is the unbalance mass from the disk and *d* is the disk unbalance eccentricity with respect to the shaft geometric center.

The rotor-bearing system described by Eq. (1) can also be expressed in state-space representation as:

$$\{\dot{x}(t)\}=[A]\{x(t)\}+[E_u]\{n_1(t)\} \tag{4}$$

where the state vector is given by

$$\{x(t)\}=\begin{Bmatrix}\xi(t)\\ \cdots\\ \dot{\xi}(t)\end{Bmatrix} \tag{5}$$

and

ISSN 2176-5480

$$\left[E_u\right] = \begin{bmatrix} 0 \\ \cdots \\ M^{-1}H \end{bmatrix} \tag{6}$$

The expression for the correlation matrix is defined by:

$$\left[R_{xx}(t, t+\tau)\right] = \left[R_{xx}(\tau)\right] = \varepsilon\left\{\left\{x(t)\right\}\left\{x^T(t+\tau)\right\}\right\} \tag{7}$$

where τ is a time delay instant and ε means the expected value between two terms.

Equations (2) and (3) can be rewritten as (Lalanne and Ferraris, 1990):

$$\left[H\right] = \begin{bmatrix} 0 & 0 \\ \vdots & \vdots \\ a\Omega^2 & b\Omega^2 \\ -b\Omega^2 & a\Omega^2 \\ 0 & 0 \\ \vdots & \vdots \\ 0 & 0 \end{bmatrix}_{(n,2)} \quad \text{with } \left\{n_1(t)\right\} = \left\{n(t)\right\} = \begin{Bmatrix} \sin(\Omega t) \\ \cos(\Omega t) \end{Bmatrix} \tag{8}$$

where

$$a = m_u d\cos\beta \quad \text{and} \quad b = m_u d\sin\beta \tag{9}$$

Applying Eq. (7) to Eq. (4) and using Eqs. (8) and (9), it is possible to obtain an equation that correlates the system outputs with the rotor fault parameters and the physical system parameters (Pederiva, 1992 and Eduardo, 2003). This equation is called *Generalized Lyapunov Matrix Equation* for systems excited by harmonic forces:

$$\left[A\right]\left[R_{xx}(\tau_i)\right] + \left[R_{xx}(\tau_i)\right]\left[A\right]^T + \left[E_u\right]\left[R_{nx}(\tau_i)\right] + \left[R_{xn}(\tau_i)\right]\left[E_u\right]^T = 0 \tag{10}$$

The above involved matrices are detailed described in Sanches and Pederiva (2011).

2.1 Reduction of the system measured outputs

All the assumptions considered previously took into consideration that the entire state vector is measured. In practice this does not occur because some degrees of freedom are not available by reasons that include safety and difficulties to access some measuring points on the machine. This way, an output measurement reduction should be considered in order to work with a more realistic situation that enables this methodology to be applied in real rotating machines.

It is known that velocity and displacement measurements are redundant considering the system observability and this represents a natural output reduction. So, with only the displacements it is possible to observe completely the system (Pederiva, 1992). The goal is not only to exclude the velocities but also to provide an addition reduction with respect to the number of displacements acquired by transducers.

Considering that the entire state vector is not available, Eq. (10) cannot be applied and additional correlations should be used to replace the missing ones.

In order to replace the missing state variables and to generate additional data to be used in the identification process, Pederiva (1992) proposes the utilization of a filter system. Figure 1 shows how the filter acts in the mechanical system.

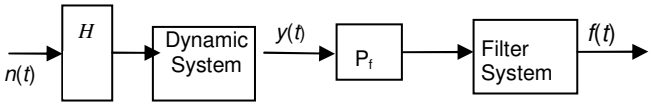

Figure 1. Schematic representation of the dynamic system + filter

ISSN 2176-5480

The filter system is represented by the state-space equation:

$$\left[\dot{f}(t)\right] = \left[N\right]\left\{f(t)\right\} + \left[P_f\right]\left\{y(t)\right\} \tag{11}$$

with:

$$\left\{f^T(t)\right\} = \left\{\eta_1 \quad \eta_2 \quad \cdots \quad \eta_q\right\}_{(1,q)} \tag{12}$$

η_1 to η_q are the filter outputs.

The filter system has order q and it is stable and controllable. The parameters n_1 to n_q are filter parameters, p_1 to p_m are the input filter parameters and the index m is the number of available measured outputs.

When a reduction of the measured state variables is performed, the system must continue to be observable by the available variables that are possible to be acquired. Dynamic systems described as showed by Eq. (4) can be represented in many different ways which are known as normal forms of state equation and these new forms have other coordinate systems, so the input/output system description changes as well as the input/output system matrices.

Through a specific coordinate base, it is possible to obtain transformed matrices $[A^*]$, $[B^*]$ and $[C^*]$ that contain simple internal structures which can be easily used in a parameter estimation algorithm. These special structures are obtained by the choice of specific coordinate transformation basis.

This way, changing the coordinate basis:

$$\left\{x^*(t)\right\} = \left[T\right]\left\{x(t)\right\} \tag{13}$$

where $[T]$ is the coordinate transformation matrix.

Performing a coordinate transformation in the studied system:

$$\left\{\dot{x}^*\right\} = \left[A^*\right]\left\{x^*(t)\right\} + \left[E^*\right]\left\{n(t)\right\} \tag{14}$$

Considering the original rotating system completely observable, it is desirable that this condition be still valid with a reduction of the output measurements. In other words, the transformation matrix should be conveniently chosen. To guarantee the system observability in the case of having some parts of the state vector, the transformation matrix used to rewrite the rotating system will be the observability matrix. So $[T]$ has the form:

$$\left[T\right]^T = \left[C \quad C.A \quad C.A^2 \quad \ldots \quad C.A^{2n-1}\right] \tag{15}$$

Applying this coordinate transformation to the rotor system, the matrices $[A^*]$ and $[C^*]$ have special structures (Pederiva, 1992) that are very useful to have an identification algorithm.

As mentioned previously a filter system is used to generate additional data to replace the missing correlations. This way the complete system is formed by the rotating system plus the filter and this *expanded system* is described by:

$$\left\{\dot{x}_e(t)\right\} = \left[A_e^{'}\right]\left\{x_e(t)\right\} + \left[E_e^{'}\right]\left\{n(t)\right\} \tag{16}$$

with

$$\left\{x_e(t)\right\} = \begin{Bmatrix} x^*(t) \\ f(t) \end{Bmatrix} \tag{17}$$

$$\left[A_e^{'}\right] = \begin{bmatrix} A^* & 0 \\ P_f C^* & N \end{bmatrix} \tag{18}$$

ISSN 2176-5480

and

$$\left[E_e^{'}\right]=\begin{bmatrix} E^{*} \\ 0 \end{bmatrix} \tag{19}$$

The Lyapunov matrix equation described by Eq. (10) can be represented in a general form to the expanded system as:

$$\left[A^{'}\right]\left[R^{'}\right]+\left[R^{'}\right]\left[A^{'}\right]^{T}=\left[Q^{'}\right] \tag{20}$$

2.2 Guyan reduction

The initial finite element discretization of a rotor system needs a relatively large number of degrees of freedom (DOFs) for satisfactory accuracy. A reduction of the number of DOFs is sometimes necessary because, in actual applications, only a few lower modes are of concern, giving little justification for solving the complete equation of motion in dynamic analysis (Rades, 2009).

The basis for the Guyan reduction is to follow a standard procedure used in static structural analysis, namely, elimination of DOFs at which no forces are applied, whence the name of *static condensation* (Guyan, 1965).

The DOFs are divided in two groups: a) the active coordinates and b) the discarded coordinates, denoted by "*a*" and "*d* ", respectively. Partitioning Eq. (1) accordingly:

$$\begin{bmatrix}\begin{bmatrix}M_{aa}\end{bmatrix} & \begin{bmatrix}M_{ad}\end{bmatrix} \\ \begin{bmatrix}M_{da}\end{bmatrix} & \begin{bmatrix}M_{dd}\end{bmatrix}\end{bmatrix}\begin{Bmatrix}\ddot{\xi}_a \\ \ddot{\xi}_d\end{Bmatrix}+\begin{bmatrix}\begin{bmatrix}P_{aa}\end{bmatrix} & \begin{bmatrix}P_{ad}\end{bmatrix} \\ \begin{bmatrix}P_{da}\end{bmatrix} & \begin{bmatrix}P_{dd}\end{bmatrix}\end{bmatrix}\begin{Bmatrix}\dot{\xi}_a \\ \dot{\xi}_d\end{Bmatrix}+\begin{bmatrix}\begin{bmatrix}K_{aa}\end{bmatrix} & \begin{bmatrix}K_{ad}\end{bmatrix} \\ \begin{bmatrix}K_{da}\end{bmatrix} & \begin{bmatrix}K_{dd}\end{bmatrix}\end{bmatrix}\begin{Bmatrix}\xi_a \\ \xi_d\end{Bmatrix}=\begin{Bmatrix}F_a \\ F_d\end{Bmatrix} \tag{21}$$

where

$$\{F\}=[H]\{n_1(t)\} \tag{22}$$

Assuming $\{F_d\}=\{0\}$, the static force-deflection relationship is given by:

$$\begin{bmatrix}\begin{bmatrix}K_{aa}\end{bmatrix} & \begin{bmatrix}K_{ad}\end{bmatrix} \\ \begin{bmatrix}K_{da}\end{bmatrix} & \begin{bmatrix}K_{dd}\end{bmatrix}\end{bmatrix}\begin{Bmatrix}\xi_a \\ \xi_d\end{Bmatrix}=\begin{Bmatrix}F_a \\ 0\end{Bmatrix} \tag{23}$$

The lower partition provides a static constraint equation:

$$\left[K_{da}\right]\{\xi_a\}+\left[K_{dd}\right]\{\xi_d\}=\{0\} \tag{24}$$

which can be written as:

$$\{\xi_d\}=-\left[K_{dd}\right]^{-1}\left[K_{da}\right]\{\xi_a\} \tag{25}$$

The original set of coordinates can be related to the subset of active or measured coordinates by the following equation:

$$\{\xi\}=\begin{Bmatrix}\xi_a \\ \xi_d\end{Bmatrix}=\begin{bmatrix} I_a \\ -\left[K_{dd}\right]^{-1}\left[K_{da}\right]\end{bmatrix}\{\xi_a\}=\left[\bar{T}\right]\{\xi_a\} \tag{26}$$

$\left[\bar{T}\right]$ is the *reduction matrix.*

The transformation in Eq. (26) is time independent, then substituting this equation in Eq. (1) and premultiplying by $\left[\bar{T}\right]^{T}$ it is possible to have a reduced equation of motion that is given in function of the active (measured) physical coordinates:

ISSN 2176-5480

$$\left[M^{red}\right]\left\{\ddot{\xi}_a(t)\right\}+\left[P^{red}\right]\left\{\dot{\xi}_a(t)\right\}+\left[K^{red}\right]\left\{\xi_a(t)\right\}=\left\{F^{red}(t)\right\} \tag{27}$$

3. ROTOR SIMULATIONS

The Jeffcott rotor was modeled by finite elements with three nodes: two of them are at the bearings position and the third one is located at the disc position. This way, the rotor system has 12 degrees of freedom: six linear coordinates and six angular ones (Lalanne and Ferraris, 1990). It will be considered that only the two linear coordinates at the disc position are available to be measured by a transducer, so only 1/12 of the state vector is known.

This level of reduction requires that the observability matrix [T] in Eq. (15) contains the system matrix [A] raised to the eleventh power. The transformed system matrix [A^*] involves [T]$^{-1}$, so these mathematical operations involve high computational costs justifying the application of model order reduction whose objective is to low the exponent of the matrix [A].

Figure (2) shows the simulated Jeffcott rotor:

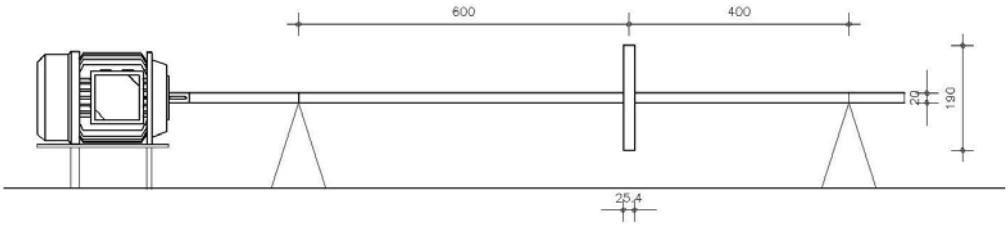

Figure 2. Simulated Jeffcott Rotor – dimensions in millimeters

The rotor is supported by two rolling bearings.

3.1 Model order reduction

As mentioned before, each node has 4 degrees of freedom and they are showed by Fig. (3) (Lalanne and Ferraris, 1990):

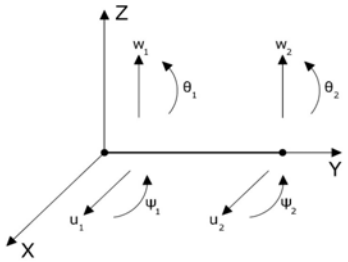

Figure 3. Shaft finite element

Considering that only the linear coordinates at the disc position are available, the active coordinates are given by:

$$\left\{\xi_a\right\}=\begin{Bmatrix} u_{disc} \\ w_{disc} \end{Bmatrix} \tag{28}$$

Reducing the system considering only the active coordinates, the *reduction matrix* is given by:

$$\left[\overline{T}\right]=\begin{bmatrix} I_{(2,2)} \\ -K_{dd}^{-1}{}_{(10,10)} \quad K_{da}{}_{(10,2)} \end{bmatrix} \tag{29}$$

Representing Eq. (27) in state space form, it follows that the reduced system has order four and ½ of the state vector is known and this brings much lower powers of the system matrix [A].

ISSN 2176-5480

This way, the observability matrix is given by:

$$[T] = \begin{bmatrix} C \\ C.A \end{bmatrix} \tag{30}$$

When one have reductions of ½ of the state vector, Pederiva (1992) shows that the observability matrix is equal to the identity matrix and it is necessary a filter of order 3 to generate an identification algorithm to estimate the fault parameters.

Details of the generation of the identification algorithm can be seen in Pederiva (1992) and Sanches and Pederiva (2010). The equation used to identify the fault parameters is:

$$-r_{\eta_3\xi} + \left\{ r_{\eta_1\xi} \quad \vdots \quad r_{\eta_2\xi} \right\} \begin{bmatrix} A_1^{*T} \\ A_2^{*T} \end{bmatrix} = Q_{3_{(1,1:2)}} \tag{31}$$

where $-r_{\eta_i\xi}$ is the correlation matrix between the ith filter output and the active (measured) coordinates. Q_3 is a sub matrix of $[Q^{'}]$ in Eq. (20) (Sanches and Pederiva, 2010).

The unbalance parameters for each disk as well as a general view of the shaft bow are showed by Fig. 4:

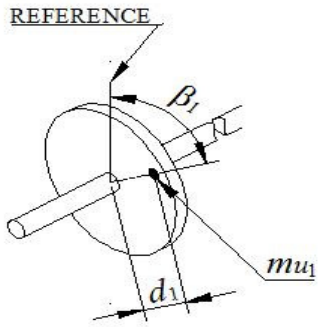

Figure 4. Representation of the disc unbalance

3.2 Numerical results

The first two natural frequencies of the studied Jeffcott rotor are shown by the Campbell diagram below:

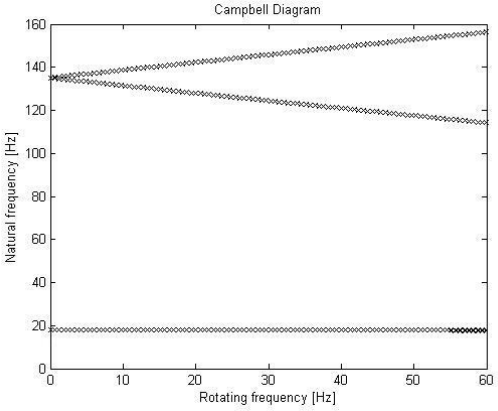

Figure 5. Campbell Diagram

As one can see on Fig. (5), the gyroscopic effect is very low at the first critical speed, but for the second critical speed this effect should be taken into account. This paper is a theoretical study and the goal is the validation in an experimental test rig. The Jeffcott rotor showed by Fig. (2) is being built and it will be controlled by a frequency

ISSN 2176-5480

inverter that has the limit of 60 Hz as the maximum rotating frequency delivered to the rotor, so the second critical speed will not be reached during the experimental running. This is the reason why simulations over 60 Hz are not performed, although these cases can be simulated without any problems.

This way, the filter system should be conveniently chosen so as not to soften any system response presented at frequency inverter operation range. Details of the third order filter can be seen in Pederiva (1992) and its first frequency is 125 Hz which is far from the first critical speed. The rotor characteristics are shown by Tabs. (1) and (2):

Table 1. Disc parameters

Mass: 5,4 kg	Material: steel
Thickness: 25,4 mm	Outer diameter: 190 mm

Table 2. Rolling bearing parameters

$K_{xx} = 8.10^5$ N/m	$C_{xx} = 10.000$ N.s/m
$K_{zz} = 8.10^5$ N/m	$C_{zz} = 10.000$ N.s/m
$K_{xz} = K_{zx} = 0$	$C_{xz} = C_{zx} = 0$

To estimate the unbalance parameters, it was used in Eq. (31) three time delays τ_i and several different rotating speeds. The unbalance will be varied in location and magnitude in order to test the ability of the identification algorithm in estimate the unbalance parameters.

Two unbalance configurations will be tested and the unbalance position will be varied in four angular positions in relation to a reference located on the disc: 60^o, 150^o, 220^o, 330^o. The table bellow shows the simulated cases:

Table 3. The unbalance cases simulated

Configuration 1	Configuration 2
$m_u d = 1{,}40.10^{-4}$ kg.m	$m_u d = 2{,}70.10^{-4}$ Kg.m

All the simulated cases are shown in the following tables, varying the number of rotating frequencies as well as the unbalance location. The number of rotating speeds used to estimate the unbalance parameters will be increased in order to add more simulated rotor responses in different dynamic situations that varies with the rotation speed.

Case 1: Simulations considering four rotating frequencies: 5, 12, 25 and 40Hz with the unbalance at 60^o from the reference. The results are showed by Tab. 4:

Table 4. Simulations using four rotating speeds

Config.1	Error (%)	Config.2	Error (%)
$m_{u1}d_1 = 1{,}42.10^{-4}$	1,43	$m_{u1}d_1 = 2{,}73.10^{-4}$	1,11
$\beta_1 = 57{,}68^0$	3,87	$\beta_1 = 57{,}68^0$	3,87

Case 2: Simulations considering eight rotating frequencies: 5, 10, 12, 25, 30, 40, 50 and 60Hz with the unbalance at 60^o from the reference. The results are showed by Tab. 5:

Table 5. Simulations using eight rotating speeds

Config.1	Error (%)	Config.2	Error (%)
$m_{u1}d_1 = 1{,}395.10^{-4}$	0,36	$m_{u1}d_1 = 2{,}69.10^{-4}$	0,37
$\beta_1 = 58{,}58^0$	2,37	$\beta_1 = 58{,}58^0$	2,37

Case 3: Simulations considering twelve rotating frequencies: 5, 10, 12, 15, 25, 30, 35, 40, 45, 50, 55 and 60Hz with the unbalance at 60^o from the reference. The results are showed by Tab. 6:

Table 6. Simulations using twelve rotating speeds

Config.1	Error (%)	Config.2	Error (%)
$m_{u1}d_1 = 1{,}396.10^{-4}$	0,29	$m_{u1}d_1 = 2{,}69.10^{-4}$	0,37
$\beta_1 = 58{,}59^0$	2,35	$\beta_1 = 58{,}59^0$	2,35

Case 4: Simulations considering four rotating frequencies: 5, 12, 25 and 40Hz with the unbalance at 150^o from the reference. The results are showed by Tab. 7:

ISSN 2176-5480

Table 7. Simulations using four rotating speeds

Config.1	Error (%)	Config.2	Error (%)
$m_{u1}d_1 = 1{,}415.10^{-4}$	1,07	$m_{u1}d_1 = 2{,}73.10^{-4}$	1,11
$\beta_1 = 147{,}68^0$	1,55	$\beta_1 = 147{,}68^0$	1,55

Case 5: Simulations considering eight rotating frequencies: 5, 10, 12, 25, 30, 40, 50 and 60Hz with the unbalance at 150^o from the reference. The results are showed by Tab. 8:

Table 8. Simulations using eight rotating speeds

Config.1	Error (%)	Config.2	Error (%)
$m_{u1}d_1 = 1{,}396.10^{-4}$	0,29	$m_{u1}d_1 = 2{,}69.10^{-4}$	0,37
$\beta_1 = 148{,}59^0$	0,94	$\beta_1 = 148{,}58^0$	0,95

Case 6: Simulations considering twelve rotating frequencies: 5, 10, 12, 15, 25, 30, 35, 40, 45, 50, 55 and 60Hz with the unbalance at 150^o from the reference. The results are showed by Tab. 9:

Table 9. Simulations using twelve rotating speeds

Config.1	Error (%)	Config.2	Error (%)
$m_{u1}d_1 = 1{,}396.10^{-4}$	0,29	$m_{u1}d_1 = 2{,}69.10^{-4}$	0,37
$\beta_1 = 148{,}59^0$	0,94	$\beta_1 = 148{,}59^0$	0,94

Case 7: Simulations considering four rotating frequencies: 5, 12, 25 and 40Hz with the unbalance at 220^o from the reference. The results are showed by Tab. 10:

Table 10. Simulations using four rotating speeds

Config.1	Error (%)	Config.2	Error (%)
$m_{u1}d_1 = 1{,}415.10^{-4}$	1,07	$m_{u1}d_1 = 2{,}73.10^{-4}$	1,11
$\beta_1 = 217{,}68^0$	1,05	$\beta_1 = 217{,}68^0$	1,05

Case 8: Simulations considering eight rotating frequencies: 5, 10, 12, 25, 30, 40, 50 and 60Hz with the unbalance at 220^o from the reference. The results are showed by Tab. 11:

Table 11. Simulations using eight rotating speeds

Config.1	Error (%)	Config.2	Error (%)
$m_{u1}d_1 = 1{,}396.10^{-4}$	0,29	$m_{u1}d_1 = 2{,}69.10^{-4}$	0,37
$\beta_1 = 218{,}58^0$	0,65	$\beta_1 = 218{,}58^0$	0,65

Case 9: Simulations considering twelve rotating frequencies: 5, 10, 12, 15, 25, 30, 35, 40, 45, 50, 55 and 60Hz with the unbalance at 220^o from the reference. The results are showed by Tab. 12:

Table 12. Simulations using twelve rotating speeds

Config.1	Error (%)	Config.2	Error (%)
$m_{u1}d_1 = 1{,}396.10^{-4}$	0,29	$m_{u1}d_1 = 2{,}69.10^{-4}$	0,37
$\beta_1 = 218{,}59^0$	0,64	$\beta_1 = 218{,}59^0$	0,64

Case 10: Simulations considering four rotating frequencies: 5, 12, 25 and 40Hz with the unbalance at 330^o from the reference. The results are showed by Tab. 13:

Table 13. Simulations using four rotating speeds

Config.1	Error (%)	Config.2	Error (%)
$m_{u1}d_1 = 1{,}415.10^{-4}$	1,07	$m_{u1}d_1 = 2{,}73.10^{-4}$	1,11
$\beta_1 = 327{,}68^0$	0,70	$\beta_1 = 327{,}68^0$	0,70

Case 11: Simulations considering eight rotating frequencies: 5, 10, 12, 25, 30, 40, 50 and 60Hz with the unbalance at 330^o from the reference. The results are showed by Tab. 14:

Table 14. Simulations using eight rotating speeds

Config.1	Error (%)	Config.2	Error (%)
$m_{u1}d_1 = 1{,}396.10^{-4}$	0,29	$m_{u1}d_1 = 2{,}69.10^{-4}$	0,37
$\beta_1 = 328{,}58^0$	0,43	$\beta_1 = 328{,}58^0$	0,43

ISSN 2176-5480

Case 12: Simulations considering twelve rotating frequencies: 5, 10, 12, 15, 25, 30, 35, 40, 45, 50, 55 and 60Hz with the unbalance at 330^o from the reference. The results are showed by Tab. 15:

Table 15. Simulations using twelve rotating speeds

Config.1	Error (%)	Config.2	Error (%)
$m_{u1}d_1 = 1{,}396.10^{-4}$	0,29	$m_{u1}d_1 = 2{,}69.10^{-4}$	0,37
$\beta_1 = 328{,}59^0$	0,43	$\beta_1 = 328{,}59^0$	0,43

4. CONCLUSIONS

The simulations performed for the Jeffcott rotor showed that is possible to use model order reduction techniques to estimate fault parameters.

It is known that the Guyan reduction is not the best method available since the damping and gyroscopic effect are present in rotating systems, but in this case, it can be used as a very good first approximation to obtain accurate unbalance parameters: magnitude and phase (location).

The simulated results are considered good and Guyan reduction has worked well because the gyroscopic effect can be neglected for rotating frequencies until the 60 Hz, which is the operating range of the frequency inverter, and the damping factor is low, about 1,41 %, considering the first vibration mode.

This is a first study involving faults estimation and model reduction techniques and the preliminary results show good perspectives in terms of combining these methods in order to identify malfunctions in rotating machines. This work will continue considering more faults and other model reduction techniques.

5. REFERENCES

Bachschmid, N., Pennacchi, P. and Vania, A., 2002. "Identification of Multiple Faults in Rotor Systems". *Journal of Sound and Vibration,* Vol. 254 (2), p. 327-366.

Eduardo, A.C., 2003. *Fault Diagnosis in Rotor Systems through Correlation Analysis and Artificial Neural Networks*. Ph.D. Thesis, Faculty of Mechanical Engineer, University of Campinas, Campinas.

Guyan, R.J., 1965. "Reduction of stiffness and mass matrices". *AIAA Journal*, Vol. 3 (2), p. 380.

Jalan, A.K. and Mohanty, A.R., 2009. "Model based fault diagnosis of a rotor-bearing system for misalignment and unbalance under steady-state condition". *Journal of Sound and Vibration*, Vol. 327, p. 604-622.

Lalanne, M. and Ferraris, G., 1990. *Rotordynamics Prediction in Engineering*. John Wiley and Sons, West Sussex, 1st edition

Lees, A.W., Sinha, J.K. and Friswell, M.I., 2009, "Model-Based Identification of Rotating Machines". *Mechanical Systems and Signal Processing*, Vol. 23, pp. 1884-1893.

Market, R., Platz, R. and Seidler, M., 2001. "Model based fault identification in rotor systems by least squares fitting". *International Journal of Rotating Machinery*, Vol. 7 (5), p. 311-321.

Pederiva, R., 1992. *Parametric Identification of Stochastically Excited Mechanical Systems*. Ph.D. Thesis, Faculty of Mechanical Engineer, University of Campinas, Campinas.

Rades, M., 2009. *Dynamics of Machinery II*. Printech, Bucharest, 1st edition.

Rao, J.S., 2001, "A Note on Jeffcott Warped Rotor". Mechanism and Machine Theory, Vol. 36, pp. 563-575.

Sanches, F.D. and Pederiva, R., 2009. "Bearing parameters estimation using correlation analysis and random response", *Proceedings of the 20th International Congress of Mechanical Engineering – COBEM2009*. Gramado, Brazil.

Sanches, F.D. and Pederiva, R., 2010. "Identification of the unbalance using correlation analysis and unbalance responses", *Proceedings of the 8th IFToMM International Conference on Rotordynamics*. Seoul, Korea.

Sanches, F.D. and Pederiva, R., 2011. "Multi faults estimation in rotor systems using correlation analysis", *Proceedings of the 21st International Congress of Mechanical Engineering – COBEM2011.* Natal, Brazil.

Sekhar, A.S., 2005. "Identification of unbalance and crack acting simultaneously in a rotor system: modal expansion versus reduced basis dynamic expansion". *Journal of Vibration and Control,* Vol. 11 (9), p. 1125-1145.

Sudhakar, G.N.D.S. and Sekhar, A.S., 2011. "Identificantion of unbalance in a rotor bearing system". *Journal of Sound and Vibration*, Vol. 330, p. 2299-2313.

Wagner, M.B., Younan, A., Allaire, P. and Cogill, R., 2010. "Model order reduction methods for rotor dynamic analysis: a survey and review". *International Journal of Rotating Machinery*, Vol. 2010, p. 1-17.

6. RESPONSIBILITY NOTICE

The authors are the only responsible for the printed material included in this paper.